

Article

# Vapor–Gas Deposition of Polymer Coatings on Metals from Azeotropic Solutions of Organosilanes

Yu. B. Makarychev

A.N. Frumkin Institute of Physical Chemistry and Electrochemistry, Russian Academy of Sciences, Leninsky pr. 31, Moscow 119071, Russia; makarychev-1949@mail.ru

**Abstract:** The mechanism of the vapor–gas deposition of vinyltrimethoxysilane (VS) and ethylene glycol (EG) from azeotropic solutions is investigated, which allows a reduction of the evaporation temperature of the components of working mixtures. The need for such studies is associated with the development of a new direction in the technology of vapor–gas deposition of polymer coatings. Methods have been developed for monitoring the chemical composition of working solutions in evaporators using optical spectroscopy, which makes it possible to calculate the partial pressures of vapor-phase components. Based on these studies, compositions of working solutions are proposed that allow the equalization of the partial pressures of the components of working mixtures with a large difference in the boiling point. With the aid of vapor–gas deposition, siloxane coatings on low-carbon steel were obtained, the protective properties of which exceeded the treatment with volatile inhibitors of the adsorption type by two to three orders of magnitude. A new method of vapor–gas deposition of non-volatile powder inhibitors on metals is proposed. Chemical compositions of siloxane coatings were determined using XPS, and mechanisms of interaction of VS with the polymerization promoters ethylene glycol and 1-hydroxy ethylidene-1,1-diphosphonic acid (HEDP) were proposed.

**Keywords:** vapor-phase deposition; organosilanes; azeotropic solutions; X-ray photoelectron spectroscopy; optical spectroscopy



**Citation:** Makarychev, Y.B.

Vapor–Gas Deposition of Polymer Coatings on Metals from Azeotropic Solutions of Organosilanes. *Surfaces* **2023**, *6*, 291–303. <https://doi.org/10.3390/surfaces6030021>

Academic Editor: Gaetano Granozzi

Received: 18 July 2023

Revised: 26 August 2023

Accepted: 27 August 2023

Published: 1 September 2023



**Copyright:** © 2023 by the author. Licensee MDPI, Basel, Switzerland. This article is an open access article distributed under the terms and conditions of the Creative Commons Attribution (CC BY) license (<https://creativecommons.org/licenses/by/4.0/>).

## 1. Introduction

Steam–gas treatment with corrosion inhibitors is widely used for the preservation of industrial products during long-term storage or transportation in conditions of high humidity and aggressive atmosphere [1–6]. The vast majority of existing volatile corrosion inhibitors are adsorption-type inhibitors (VCIA) based on aliphatic carboxylic acids and amines. As a rule, these are monofunctional compounds, having in their composition a carboxylic R=CO(OH) or an amine R-NH<sub>2</sub> group of atoms through which a chemical bond with a metal is carried out. Such compounds form monolayer coatings that prevent the adsorption of aggressive substances on the surface of metals; however, they do not have the high barrier and mechanical properties required to protect against corrosion in conditions of long-term storage, high temperature and humidity. A distinctive feature of VCI is the selective chemisorption of molecules on various metals. Amine-based inhibitors are effective for metals that have free d-orbitals (Fe, Cu, Zn) that are capable of forming donor-acceptor bonds [7–9] with an unshared pair of nitrogen electrons. Compounds containing a carboxyl group of atoms form strong chemical bonds with hydroxylated surfaces of light metals (Al, Mg) as a result of the condensation reaction of acid protons and hydroxyl groups on the metal's surface [10,11]. Volatile polymer-type corrosion inhibitors (VCIP) based on organosilanes can form a polymer coating on the surface of any metals [12–14] and mineral substrates with the formation of strong chemical bonds. Most VCIA compounds have low partial pressures at deposition temperatures of 10<sup>-7</sup>–10<sup>-5</sup>, which significantly reduces the rate of inhibitor deposition. VCIP partial pressures can be varied over any atmospheric pressure range due to the use of azeotropic mixtures. This makes it possible to obtain

polymer layers hundreds of nanometers thick on metal surfaces in a short time and at relatively low temperatures. Currently, there are a large number of organosilanes suitable for vapor–gas deposition on metals. The main condition is the presence of the  $-\text{Si}(\text{OR})_3$  groups of atoms in organic compounds. This greatly facilitates the preparation of inhibitory compositions for obtaining polymer coatings with desired properties. Our studies [14] have shown that the polymerization rate of silanols increases significantly in the presence of multifunctional aliphatic, carboxylic and phosphonic acids. The most suitable for these purposes is ethylene glycol, which has two groups in its composition  $-\text{OH}$ , capable of participating in the polycondensation reactions with VS molecules. In this connection, vinyltrimethoxysilane (VS) and ethylene glycol (EG) were chosen as the main components of polymer mixtures. The technology of the deposition of VS in the gas phase can be used for the deposition of powder corrosion inhibitors on metals that have extremely low vapor pressures at operating temperatures of 100–150 °C. The possibility of precipitation of HEDP and 1.2.3 benzotriazole (BTA) on steel from organic solutions together with VS has been investigated. It was found that solutions of HEDP in ethanol and BTA in isopropanol evaporate azeotropically during boiling in a wide range of concentrations. The role of organosilanes is to cross-link the inhibitor molecules with VS molecules during their joint deposition on the surface of metals. The subject of this present research is the study of the vapor–gas deposition mechanism of VS and powder inhibitors on the iron surface using the XPS and optical spectroscopy methods. Based on the obtained research results, we developed optimal technologies for the deposition of VS with polymerization promoters and powder coatings with high barrier properties.

## 2. Experimental Procedure

### 2.1. Materials and Solutions

The following materials were used for steam–gas deposition  
 -Vinyltrimethoxysilane (VS), (Witco Co);  $\text{CH}_2 = \text{CH} - \text{Si}(\text{OCH}_3)_3$   
 -Ethylene Glycol (EG), (Chem.Avangard);  $\text{HO}-\text{CH}_2-\text{CH}_2-\text{OH}$   
 -1-Hydroxy Ethylidene-1,1-Diphosphonic Acid (HEDP), (Chem.Rus)  $\text{CH}_3\text{C}(\text{OH})(\text{H}_2\text{PO}_3)_2$   
 -1.2.3 Benzotriazole (BTA), (Chem.Russia);  $\text{C}_6\text{H}_5\text{N}_3$   
 -Butanol (Bt), (Chem.Russia);  $\text{C}_4\text{H}_9\text{OH}$   
 -Phenylmethane (Ph), (Chem.Russia);  $\text{C}_6\text{H}_5\text{CH}_3$   
 -Isopropanol (IPA),  $\text{C}_3\text{H}_8\text{OH}$  (Chem.Avangard)

### 2.2. Surface Treatment of Samples before Research

Samples of St.3 carbon steel were used in this work (Table 1).

**Table 1.** Chemical composition%. State standard (380–2005).

C	Si	Mn	Ni	S	P	Cr	N	Cu
0.14–0.22	0.15–0.3	0.4–0.65	0.3	0.05	0.04	0.3	0.008	0.3

Before deposition of the siloxane coating, samples of 40 mm × 50 mm were sanded with SiC 400, 600, and 1000 sandpapers and then washed in acetone and distilled water. After coating, the samples were pre-cleaned in flowing water and ultrasonically cleaned in bi-distilled water before the XPS studies were conducted.

### 2.3. Deposition of Polymer Coatings from the Vapor–Gas Phase

The vapor–gas precipitation was carried out in a sealed 3 L chamber equipped with two thermometers and a disk heater to evaporate the working solutions in the measuring cylinders.

1. Sample;
2. Measuring cylinders;
3. Disk heater;

4. Thermometer 1;

5. Thermometer 2.

The azeotropic mixtures were placed in measuring cylinders. The amount of liquids in the cylinders was measured before and after the steam treatment of the samples. The temperature on the sample's surface was measured using a T4 thermometer, and the azeotropic mixture was measured with a T5 thermometer.

### 2.3.1. Optical Research

Optical studies were carried out using an AvaSpec-256 spectrophotometer. The range of wavelengths studied was 200–1160 nm, with an optical resolution of 0.5–6.4 nm. The source of radiation was a UV lamp with an excitation wavelength of 400.2 nm and radiation intensity of 743 mW/cm<sup>2</sup>. The absorption spectra of the components of the mixtures were obtained in optical glass cuvettes (Chem.Rus). The fluorescence of the polymer coatings was studied on a spectrometer in Scope mode on the mirror-polished samples of 3 cm × 5 cm in size. Chemically, the composition and thickness of the coating were evaluated by calibration absorption spectra and XPS analysis methods.

### 2.3.2. X-ray Photoelectron Spectroscopy Study

XPS measurements were performed using the OMICRON ESCA + spectrometer (Omicron NanoTechnology, Taunusstein, Germany) with the Al-anode (radiation energy 1486.6 eV; power 252 W). The pass energy of the analyzer was set at 20 eV and, in some cases, at 10 eV to increase the resolution. To take into account the charge of the samples, the position of the XPS peaks was standardized by the C1S peak of the hydrocarbon impurities from the atmosphere, in which the binding energy  $E_b$  was taken equal to 285.0 eV. The base pressure in the analyzer chamber was kept no higher than  $8 \times 10^{-10}$  mbar. The spectra were deconvoluted into components after subtraction of the background, determined by the Shirley method [15]. The element ratios were calculated using integral intensities under the peaks, taking into account the photoionization cross-sections of the corresponding electron shells [16]. Using the integrated intensity of the peaks and the MultiQuant program [17], the thicknesses of the layers formed on the surface were calculated with allowance for the mean free path of the electrons, according to the Cumpson and Seah equation [18].

## 3. Experimental Section

### 3.1. Optical Research

The chemical activity of VS is determined by the presence of three methoxy groups on the atom of silicon atoms, which are easily hydrolyzed to form  $\text{RSi(OH)}_3$  silanols. As a result of the polycondensation reaction, a chemisorption monolayer with a strong chemical bond is formed.

$\text{Me-O-Si-R(OH)}_2$  is formed on the hydroxylated surface of metals. Subsequent layers form three-dimensional cyclic siloxane structures  $[-\text{O-SiR}_2-\text{O}]_n$ , which are the basis of the polymer coating. Thus, for the polymerization of organosilanes from the vapor-gas phase on metal surfaces, the hydrolysis and polycondensation reactions must proceed sequentially. In this mechanism of polymerization, it is necessary to have two evaporators (Figure 1) for water and VS molecules in the deposition chamber (DC). Since the boiling points of water and VS differ by an order of magnitude, it is necessary to use azeotropic mixtures to equalize their partial pressures in the chamber. According to [19], such a mixture can be a 40–45% solution of VS in butane (Bt). Optical spectroscopy was used to determine the concentration of butanol in water. Figure 2 shows the calibration absorption spectra of a 40% solution of VS in butanol (a) after holding the solution in the evaporator for 30 min at  $T = 110^\circ\text{C}$  (b).

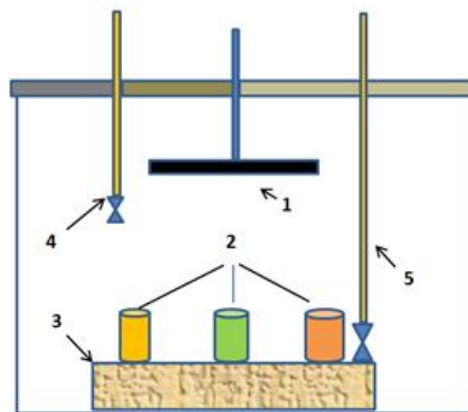


Figure 1. Coating chamber.

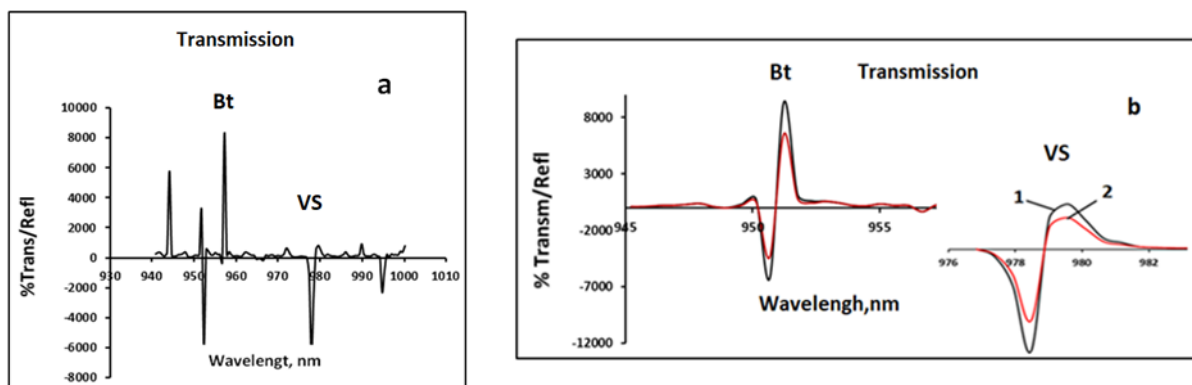


Figure 2. Calibration spectra of 60% VS solution in butanol (a) on spectra; (b) 1: initial solution; 2: after 60 min of exposure at  $T = 110\text{ }^{\circ}\text{C}$ .

As a result of the evaporation of the solution, the concentration of the initial components changes. Table 2 shows the data on the mass loss of the substance after holding the solution in the evaporator for 60 min at  $E = 110\text{ }^{\circ}\text{C}$ .

Table 2. Loss of mass of the substance after holding the solution in the evaporator.

Chemical Compound	Wavelength, nm	Intensity of the Initial Spectrum, % Transm/Refl	Spectrum Intensity after Evaporation, % Transm/Refl	Mass Loss of Substance, % vol
VS 60%	978.5	8260	6240	33.2
Bt 40%	956.4	6940	4260	39.6

From the data given in the table, it can be seen that the evaporation of the components from the solution occurs in almost an equivalent amount; that is, its composition is close to being anisotropic.

When siloxane coatings are deposited on metals from aqueous solutions, various additives in the form of corrosion inhibitors and promoters accelerating the polymerization of organosilanes are used to improve their protective properties. Only inhibitors containing at least two hydroxyl groups of atoms capable of participating in polycondensation reactions are suitable for the formation of a siloxane coating from aqueous solutions. Monofunctional inhibitors are suppressors of chains of polymer structures and interfere with the polymerization of trialkosilanes. For iron, 1-hydroxy ethylidene-1,1-diphosphonic acid (HEDP), ethylene glycol (EG) and 1.2.3 benzotriazole (BTA) can be effective promoters and corrosion inhibitors. The most suitable promoter for VS vapor deposition may be ethylene glycol

since it is a liquid of a simple chemical structure and is widely available. However, its high boiling point of 198 °C makes it difficult to use in combination with aqueous compositions. According to [20], ethylene glycol with toluene forms an azeotropic mixture with a boiling point of 110.8, while the concentration of EG in vapors is 8%. In this connection, there is a possibility of equalization of the partial pressures of vapors of water, VS and ethylene glycol in the deposition chamber (DC) during the vapor–gas deposition of siloxane coatings. In order to lower the boiling point of the mixture and increase the concentration of EC in the vapors, a mixture of 40% EG + 60% Ph/was selected.

Optical spectroscopy was used to determine the concentration of the components of the working mixtures. Figure 3 shows the calibration curves that were used for the calculations.

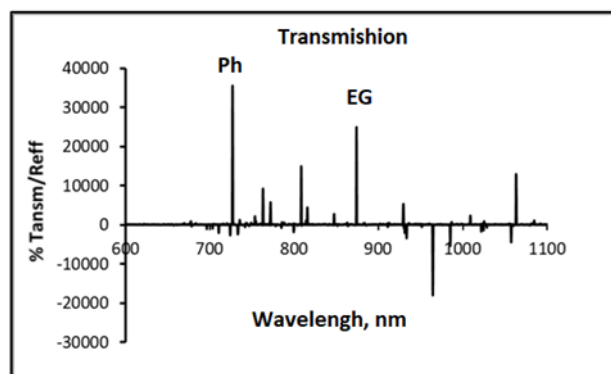


**Figure 3.** Calibration absorption spectra of a solution containing 60%Ph + 40%EG.

Table 3 shows the data on the loss of EG and phenol in evaporators during the vapor–gas deposition of VS at  $T = 110^{\circ}\text{C}$  and 60 min of deposition.

**Table 3.** Loss of mass of the substance after holding the solution in the evaporator.

Chemical Compound	Wavelength, nm	Intensity of the Initial Spectrum % Transm/Refl	Spectrum Intensity after Evaporation % Transm/Refl	Mass Loss of Substance, % vol
EG (40%)	882.3	20,560	15,740	22.5
Ph (60%)	726.4	34,520	18,630	45.1

As can be seen from the results given in Table 3, the content of EG in the vapor phase is ~40%.

Due to the fact that the temperature of the coating deposition is higher than 110 °C, ethylene glycol in the amount of 60% vol is added to the evaporator with water. According to [21], at these temperatures, the vapor phase of this mixture contains 90–95% water. Table 4 shows the composition of the working solutions in evaporators and the partial pressures of VS and EG in the deposition chamber at  $T = 110^{\circ}\text{C}$  and 60 min of deposition time.

**Table 4.** Compositions of working solutions in evaporators and partial pressures of VS and EG in the deposition chamber at  $T = 110^{\circ}\text{C}$ .

Vaporizers	Boiling Point, °C	Losses of the Components of the Mixture m, g	Partial Pressures P, at.
1. VS (60%) + Bt	106.2	2.52	0.26
2. EG (40%) + Ph	104.5	1.62	0.16
3. H <sub>2</sub> O (40%) + EG	102.8	5.8	0.63

Partial pressures  $P$  in the deposition chamber were calculated using the Mendeleev–Clapeyron formula as follows:

$$P = mRT/\mu V = n \times 0.0821 \times T/V \quad (1)$$

where  $\mu$  is the molar mass of the substance, g;  $m$  is the loss of the substance in the evaporator, g;  $n$  is the molar fraction of the substance;  $V$  is the volume of the chamber, L.

The saturated vapor pressure of ethylene glycol and VS at  $T = 110^\circ\text{C}$ , according to [22], is  $10^{-3}$ – $10^{-4}$  atm, which is about three orders of magnitude less than the pressure in the deposition chamber during the deposition of polymer coatings. It is clear that without the use of azeotropic solutions, it is impossible to obtain polymer coatings on metals with the help of the vapor–gas deposition of organosilanes.

### 3.2. XPS Research

#### 3.2.1. Studies of Vapor–Gas Deposition of VS on St.3 in a Two-Component Mixture of VS + H<sub>2</sub>O

Vapor–gas deposition was carried out at atmospheric pressure for 60 min at  $T = 110^\circ\text{C}$ . The vapor–gas mixture was obtained from two evaporators, the composition of which is given in Table 4 (p.1 and p.3).

The chemical composition of the surface of the samples was studied after coating, ultrasonic cleaning in distilled water, and air drying. Table 5 shows the chemical composition of the siloxane coating obtained from the vapor–gas phase in VS + H<sub>2</sub>O.

**Table 5.** Chemical composition of siloxane coating obtained from the vapor–gas phase in VS + H<sub>2</sub>O.

Composition of Mixtures	Si, % at	C, % at	Fe, % at	O, % at
VS + H <sub>2</sub> O	11.4	52.1	3.1	33.4

Significant amounts of silicon and carbon atoms belonging to the deposited organosilane films were detected on the X-ray spectra of the samples. In addition, a small amount of iron hydroxides was present in the composition of the coating. Figure 4 shows the XPS spectra of Si2p, on which two peaks can be distinguished, which belong to the silanol and siloxane groups of the polymer coating.

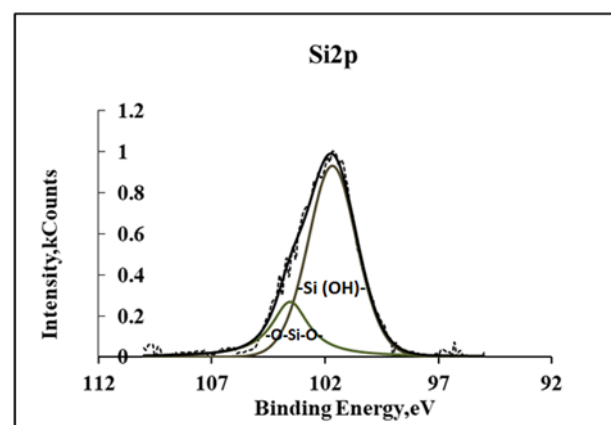


**Figure 4.** XPS spectra of Si2p siloxane coating deposited from a vapor–gas mixture of VS + H<sub>2</sub>O at  $T = 110^\circ\text{C}$ .

From these spectra, it can be seen that a significant number of silanol groups did not participate in the polymerization of the coating. On the O1s spectra (Figure 5), three peaks can be distinguished related to the silanol in VS, siloxane structures and water molecules, respectively.

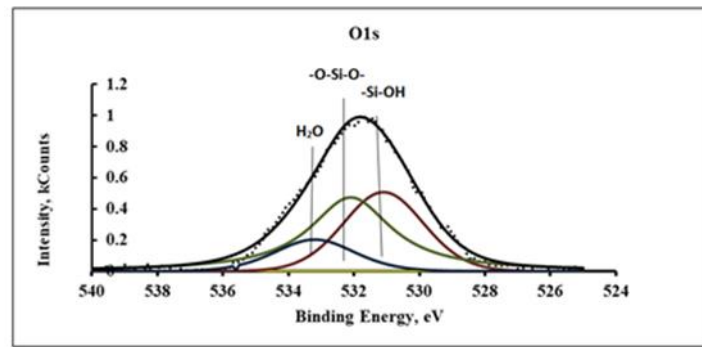


**Figure 5.** XPS spectra of O1s siloxane coating deposited from a vapor–gas mixture of VS + H<sub>2</sub>O at T = 110 °C.

It can be seen from the spectra shown in Figure 5 that the composition of the siloxane coating includes significant amounts of silanols and water. After annealing in the furnace at T = 150 °C for 60 min, the final polymerization of the coating occurs with the formation of cyclic siloxane structures, the spectra of which are shown in Figure 6.

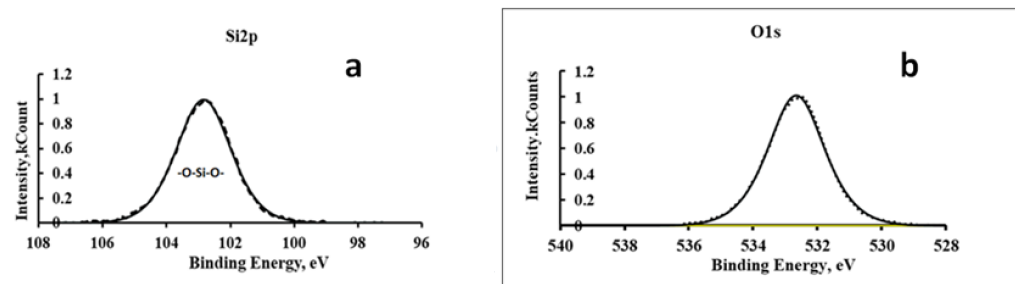


**Figure 6.** XPS spectra of Si2p (a) and O1s (b) siloxane coating after annealing in the furnace at T = 150 °C for 60 min.

Two symmetrical peaks of silicon and oxygen belonging to siloxane coating structures are visible on this spectrum.

### 3.2.2. Studies of Vapor–Gas Deposition of VS on St.3 in a Three-Component Mixture of VS + EG + H<sub>2</sub>O

Vapor–gas deposition was carried out from three evaporators at T = 110 °C for 60 min. The composition of the mixture in the evaporators is shown in Table 3. Figure 7 shows the XPS spectra of the Si2p siloxane coating.

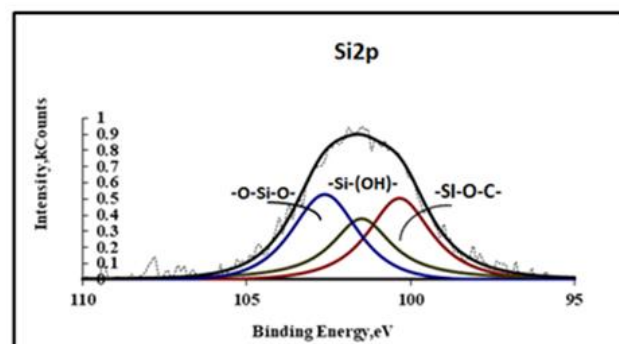


**Figure 7.** XPS spectra of Si2p siloxane coating deposited from a vapor–gas mixture in VS + EG + H<sub>2</sub>O at T = 110 °C.

In these spectra, in addition to the silanol and siloxane structures, there is a peak with an energy of 101.6 eV belonging to the silicon atoms chemically bound to ethylene glycol molecules. Ethylene glycol, having two functional groups of atoms at the end of the molecule, forms bridging bonds between the molecules, contributing to the polymerization of the siloxane coating.

When comparing the peaks on the spectrum, it can be seen that the number of silicon atoms associated with siloxane structures and ethylene glycol is approximately the same. This indicates the high chemical activity of ethylene glycol during the polymerization of the siloxane coating. The number of free silanol groups in the coating is significantly less than in the absence of ethylene glycol. This is also facilitated by higher vapor–gas deposition temperatures.

On the C1S spectra (Figure 8), ethylene glycol molecules can include a peak with an energy of 288.2 eV belonging to carbon in the C–OH groups. In the structural diagram (Figure 9), it is designated as a C3 atom.

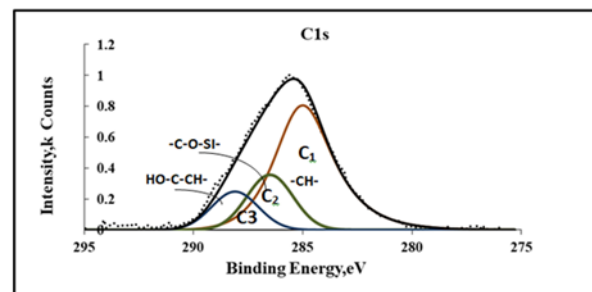


**Figure 8.** XPS spectra of C1S siloxane coating deposited from a vapor–phase mixture of VS + EG + H<sub>2</sub>O at T = 110 °C.

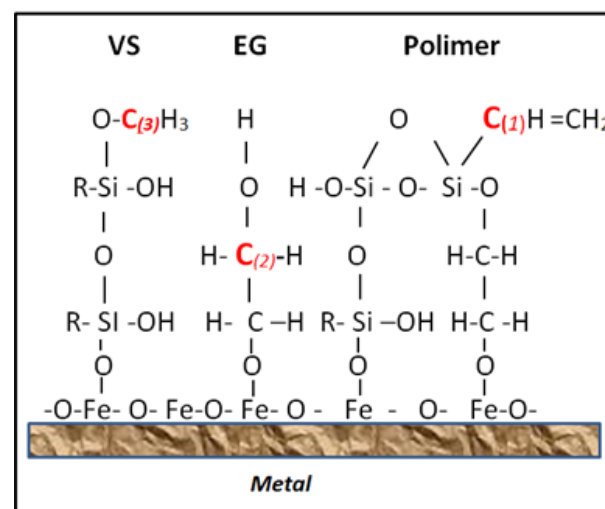


**Figure 9.** Structural diagram of a siloxane coating on the surface of steel obtained in a vapor–gas mixture of VS + EG.

The presence of methoxy groups in VS (C2) and ethoxy groups EG (C3) in the coating indicates an incomplete hydrolysis and condensation of the VS + EG molecules during precipitation. During high-temperature annealing, further polymerization of the siloxane coating occurs as a result of the condensation of the remaining hydroxy structures. Figure 9 shows the structural scheme of the siloxane coating on the surface of steel obtained in a vapor–gas mixture of VS + EG.



### 3.2.3. Investigation of Vapor–Gas Deposition of VS with Powder Inhibitors

Cyclic azoles and phosphonic acids are widely used as volatile corrosion inhibitors of metals. The authors [12,23] conducted studies on the vapor–gas deposition of phosphonic acids on low-carbon steel and magnesium alloys. In [24–29], the vapor deposition of BTA on copper, aluminum and magnesium alloys was conducted. In all cases, the thickness of the coatings was several monolayers. Obviously, the barrier properties of such coatings are not great. The ohmic resistance of charge transfer through such films is usually 1–10 kOhm [30], which is several orders of magnitude less than that of siloxal coatings [12,14]. In this regard, it is of interest to co-precipitate these inhibitors with VS to form a composite coating with increased barrier properties. The powder inhibitors BTA and HEDP have low vapor pressures of  $\sim 10^{-7}$ – $10^{-8}$ ; therefore, it is necessary to convert them into such a state that will reduce the evaporation temperature. Such a possibility can be realized if the evaporation is carried out using aqueous or organic solutions. The vapor–gas deposition of BTA and HEDP on iron from the solutions of these inhibitors in isopropanol (IPA) was investigated. The deposition was carried out using two sources, and the composition of working mixtures is provided in Table 6.

**Table 6.** The composition of the working mixtures in the evaporators.

Inhibitor	Evaporator 1	Evaporator 2	Inhibitor Concentration in IPA, M/L	Temperature in Evaporators, °C
HEDP	60% VS + 40% Bt	HEDP + (80% IPA + 20% H <sub>2</sub> O)	0.1	95
BTA	60% VS + 40% Bt	BTA + (80% IPA + 20% H <sub>2</sub> O)	0.1	95

Preliminary studies have shown that no precipitate is formed during the evaporation of the BTA and HEDP solutions, i.e., the inhibitors are completely evaporated during vapor deposition. The XPS studies showed that in the absence of VS during the vapor deposition of BTA and HEDP, thin, loose layers weakly bound to the surface of iron are formed on the iron's surface. In the presence of VS, siloxane coatings containing significant amounts of HEDP and BTA are formed. The chemical composition of these coatings is provided in Table 7.

**Table 7.** Chemical composition of siloxane coatings deposited from VS + HEDP and VS + BTA vapors.

Coating Composition	Si, % at	P, % at	C, % at	N, % at	O, % at
VS + HEDP	9.2	6.1	43.6		42.1
VS + BTA	10.4		44.7	5.5	39.4

A significant number of inhibitors in the coating is due to the fact that they are polymerization promoters and are actively embedded in the siloxane lattice, as shown in the structural diagram of Figure 10.

Using optical spectroscopy, the thicknesses of the siloxane coatings obtained by the vapor–gas deposition of VS with and without polymerization promoters were determined. Intense peaks associated with the fluorescence of the siloxane coatings were detected on the spectra of samples obtained in the Scope mode. The intensity of these peaks directly depends on the thickness of the coatings. Figure 11 shows the fluorescence spectra of the siloxane coatings on iron obtained by the vapor–gas deposition of VS with additives of the polymerization promoters EG, HEDP and BTA.

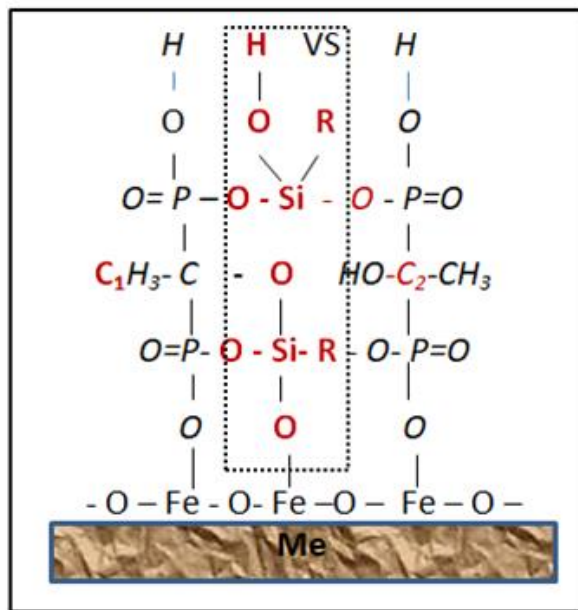


Figure 10. Structural model of siloxane coating with HEDP.

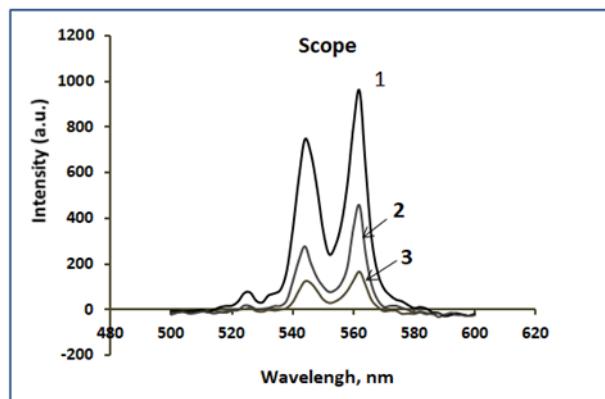


Figure 11. Fluorescence spectra of siloxane coatings on iron obtained by vapor–gas deposition of VS with additives of polymerization promoters: 1—EG; 2—HEDP; 3—BTA.

Table 8 shows the compositions of vapor–gas mixtures and the conditions for the deposition of siloxane and composite coatings.

Table 8. Compositions of vapor–gas mixtures and conditions for deposition siloxane and composite coatings.

Steam–Gas Mixture	Deposition Temperature, °C	Deposition, Time min	Coating Thickness, nm
VS + H <sub>2</sub> O	110	60	110 ± 10
VS + EG + H <sub>2</sub> O	110	60	450 ± 50
HEDP +IPA + H <sub>2</sub> O	95	60	210 ± 10
BTA +IPA + H <sub>2</sub> O	95	60	120 ± 10

From the above results, it can be seen that the most effective promoters of VS polymerization are EG, which has two active functional groups of atoms. BTA has little effect on the deposition rate of siloxane coatings; however, it is an effective corrosion inhibitor, especially for copper.

#### 4. Results and Discussion

The above studies are a continuation of a series of articles published by us over the past 2 years. They are devoted to the development of a fundamentally new direction in the inhibition of metals by steam–gas deposition of polymer siloxane coatings. Organosilanes are widely used as polymer-type corrosion inhibitors in aqueous solutions. However, they are rarely used as volatile inhibitors. The authors [2,31] investigated the mechanism of vapor–gas deposition of vinyltrimethoxysilane on aluminum, in [2] on copper, and in [32] on low-carbon steel, and in all cases, a monolayer of chemisorbed VS molecules with low barrier properties was formed on the metal surfaces. The formation of any three-dimensional phase films or polymer layers was not observed. A necessary condition for the formation of polymer siloxane coatings on metals is the presence of water molecules in the vapor–gas phase for the hydrolysis and polycondensation of silanols. The partial vapor pressures of organosilanes at the boiling point of water differ by five to six orders of magnitude; therefore, their joint deposition from separate evaporators does not lead to the formation of polymer coatings. The method of vapor–gas deposition of vinyltrimethoxysilane from the azeotropic solutions proposed in this work makes it possible to obtain polymer coatings on metals with high barrier properties. Table 9 shows the ohmic resistance of charge transfer through siloxane coatings and films of a number of adsorbed volatile inhibitors.

**Table 9.** Ohmic resistance of charge transfer through films deposited on the surfaces of the most well-known volatile metals inhibitors.

Volatile Inhibitor	Ohmic Resistance of t Stearic Acids he Coating Rcoat, kΩ·cm <sup>2</sup>	References
VS + Strodex 110	740.0	[12]
Stearic acids	7.8	[3]
2-mercaptobenzimidazole	2.67	[20]
BTA on Mg	1.6	[30]

As can be seen from the data in Table 8, the barrier properties of the siloxane polymer coatings are several orders of magnitude higher than the inhibitors of the adsorption type. In [30], studies of the vapor–gas deposition of chlorobenzotriazole on magnesium were carried out. This powder inhibitor is close to BTA in its properties. The deposition was carried out in a sealed chamber at T = 150 °C for 60 min. With the help of XPS, it was found that during this time, only a chemisorbed monolayer of chlorobenzotriazole was formed on the magnesium surface, the barrier properties of which are shown in Table 8. The vapor–gas deposition of 1,2,3-benzotriazole on steel and copper was studied in [24–28]. Studies have also been conducted on the vapor–gas deposition of phosphonic acid HEDP on low-carbon steels [12] and magnesium alloys [23]. These compounds are effective inhibitors in aqueous solutions; however, volatile inhibitors are rarely used since they do not form sufficiently dense phase films with high barrier properties. In addition, they are volatile corrosion inhibitors with extremely low partial vapor pressures. In this work, studies were conducted, and a method of vapor–gas deposition of inhibitors from alcohol solutions together with vinyltrimethoxysilane was proposed. Unlike adsorption-type inhibitors, a sufficiently thick layer of BTA and HEDP with strong intermolecular bonds is formed on the surface of metals. The role of the VS molecules is to cross-link individual inhibitor molecules into spatial three-dimensional structures.

#### 5. Conclusions

As a result of the conducted research, the compositions of azeotropic mixtures were developed to equalize the partial pressures of the components of the vapor phase during the deposition of vinyltrimethoxysilane on low-carbon steel St.3. A method for determining the partial pressures of the vapor phase using optical spectroscopy of the components of working mixtures has been developed. The main factors influencing the kinetics of the steam–gas deposition of vinyltrimethoxysilane on St.3 were determined using XPS

and optical spectroscopy. It has been found that the addition of ethylene glycol and phosphonic acid HEDP to the vapor phase of vinyltrimethoxysilane significantly accelerates the polymerization of organosilanes on the surface of metals. Using structural models, the interaction of VS with polymerization promoters is explained. A new method of vapor–gas deposition of non-volatile powder inhibitors on metals is proposed. Studies of the steam–gas deposition of the most well-known powder corrosion inhibitors, BTA and HEDP, on iron have been carried out. It has been established that BTA and HEDP dissolved in organic solvents are transferred to the metal surface during evaporation in the form of chemisorbed and Van der Waals layers with a thickness of several nanometers. To obtain dense-structured films of BTA and HEDP on the surface of metals, a technique for cross-linking Van der Waals layers with siloxanes during their joint deposition with VS has been developed.

**Funding:** This research received no external funding.

**Conflicts of Interest:** The author declares no conflict of interest.

## References

1. Sugimura, H.; Hozumi, A.; Kameyama, T.; Takai, O. Organosilane self-assembled monolayers formed at the vapour/solid interface. *Surf. Interface Anal.* **2002**, *34*, 550–554. [[CrossRef](#)]
2. Petrunin, M.A.; Maksaeva, L.B.; Yurasova, T.A.; Terekhova, E.V.; Kotenev, V.A.; Kablov, E.N.; Tsivadze, A.Y. The directional formation and protective effect of selfassembling vinyl siloxane nanolayers on copper surface. *J. Prot. Met. Phys. Chem. Surf.* **2012**, *48*, 656–664. [[CrossRef](#)]
3. Goncharova, O.A.; Luchkin, A.Y.; Archipushkin, I.A.; Andreev, N.N. Vapor-phase protection of steel by inhibitors based on salts of higher carboxylic acids. *Int. J. Corros. Scale Inhib.* **2019**, *8*, 586–599. [[CrossRef](#)]
4. Luchkin, A.Y.; Goncharova, O.A.; Andreev, N.N.; Kuznetsov, Y.I. Steel protection by treatment by vapors of octadecylamine, benzotriazole and their mixture at elevated temperature. *Koroz. Mater. Zashch. (Corros. Mater. Prot.)* **2017**, 20–27. (In Russian)
5. Zhang, D.; An, Z.; Pan, Q.; Gao, L.; Zhou, G. Volatile corrosion inhibitor film formation on carbon steel surface and its inhibition effect on the atmospheric corrosion of carbon steel. *Appl. Surf. Sci.* **2006**, *253*, 1343–1348. [[CrossRef](#)]
6. Saini, V.; Kumar, H. Study of amine as vapour phase corrosion inhibitors for mild steel under different aggressive atmospheric conditions at high temperature. *Int. J. Eng. Technol.* **2014**, *3*, 248–256.
7. Kuznetsov, Y.; Goncharova, O.; Luchkin, A.; Vesely, S.; Andreev, N. Vapor-phase protection of metals from atmospheric corrosion by low-volatile organic inhibitors, Eurocorr. In Proceedings of the European Corrosion Congress (EUROCORR 2018), Krakow, Poland, 9–13 September 2018.
8. Altsybeeva, A.I.; Burlov, V.V.; Fedorova, N.S.; Kuzinova, T.M.; Palatik, G.F. Volatile inhibitors of atmospheric corrosion of ferrous and nonferrous metals. I. Physical and chemical aspects of selection of starting reagents and synthetic routes. *Int. J. Corros. Scale Inhib.* **2012**, *1*, 51–64. [[CrossRef](#)]
9. Bastidas, D.M.; Cano, E.; Mora, E.M. Volatile corrosion inhibitors: An overview. *Anti-Corros. Methods Mater.* **2005**, *52*, 71–77. [[CrossRef](#)]
10. Hu, R.; Zhang, S.; Bu, J.; Lin, C.; Song, G. Recent progress in corrosion protection of magnesium alloys by organic coatings. *Prog. Org. Coat.* **2012**, *73*, 129–141. [[CrossRef](#)]
11. Andreeva, N.P.; Kuznetsov, Y.I.; Shikhaliev, K.S. The use of ellipsometry for studying the adsorption of organic corrosion inhibitors from aqueous solutions on metals. Review. Part 2. Adsorption of salts of organic acids and azoles. *Int. J. Corros. Scale Inhib.* **2023**, *12*, 560–585.
12. Makarychev, Y.B.; Luchkin, A.Y.; Grafov, O.Y.; Andreev, N.N. Vapor-phase deposition of polymer siloxane coatings on the surface of copper and low-carbon steel. *Int. J. Corros. Scale Inhib.* **2022**, *11*, 980–1000.
13. Yu, B.M. Vapor-Gas Deposition of Polymer Coatings on Metals and Mineral Carriers. *J. Biomed. Res. Environ. Sci.* **2022**, *3*, 1567–1569. [[CrossRef](#)]
14. Gladkikh, N.; Makarychev, Y.; Maleeva, M.; Petrunin, M.; Maksaeva, L.; Marshakov, A.; Kuznetsov, Y. Synthesis of thin organic layers containing silane coupling agents and azole on the surface of mild steel. Synergism of inhibitors for corrosion protection of underground pipelines. *Prog. Org. Coat.* **2019**, *132*, 481–489. [[CrossRef](#)]
15. Shirley, D.A. High-resolution X-ray photoemission spectrum of the valence bands of gold. *Phys. Rev. B* **1972**, *5*, 4709–4713. [[CrossRef](#)]
16. Mohai, M. XPS MultiQuant: Multimodel XPS quantification software. *Surf. Interface Anal.* **2004**, *36*, 828–832. [[CrossRef](#)]
17. Waldo, R.A. *An Iteration Procedure to Calculate Film Compositions and Thicknesses in Electron-Probe Microanalysis*; San Francisco Press: San-Francisco, CA, USA, 1988.
18. Mohai, M.; Bertoti, I. Calculation of overlayer thickness on curved surfaces based on XPS intensities. *Surf. Interface Anal.* **2004**, *36*, 805–808. [[CrossRef](#)]

19. Ageev, E.P. Azeotropic mixtures. In *Big Russian Encyclopedia [Electronic Resource]*; Chemistry, L.; 2016; p. 432.
20. Ogorodnikov, S.K.; Lesteva, T.M.; Kogan, V.B. Azeotropic Mixtures: Handbook. Chemistry, L. 1971; 847p. Available online: [https://scholar.google.com/hk/scholar?hl=zh-CN&as\\_sdt=0%2C5&q=Sergej+Kirillovi%C4%8D+Ogorodnikov&btnG=](https://scholar.google.com/hk/scholar?hl=zh-CN&as_sdt=0%2C5&q=Sergej+Kirillovi%C4%8D+Ogorodnikov&btnG=) (accessed on 26 August 2023).
21. Malenko, Y.I.; Molodnsko, P.Y. Diagrams of three-component azeotropic systems. In *Azeotropic Mixtures: Handbook*; Chemistry, L.; 1975; p. 231.
22. Lyubitov, Y.N. Saturated steam. In *Physical Encyclopedia*; Chemistry, L.; 1992; p. 84.
23. Ishizaki, T.; Okido, M.; Masuda, Y.; Saito, N.; Sakamoto, M. Corrosion Resistant Performances of Alkanoic and Phosphonic Acids Derived Self-Assembled Monolayers on Magnesium Alloy AZ31 by Vapor-Phase Method. *Langmuir* **2011**, *27*, 6009–6017. [[CrossRef](#)] [[PubMed](#)]
24. Goncharova, O.A.; Andreev, N.N.; Luchkin, A.Y.; Kuznetsov, Y.I.; Andreeva, N.P.; Vesely, S.S. Protection of copper by treatment with hot vapors of octadecylamine, 1,2,3-benzotriazole, and their mixtures. *Mater. Corros.* **2018**, *70*, 161–168.
25. Zhang, H.-L.; Zhang, D.-Q.; Gao, L.-X.; Liu, Y.-Y.; Yan, H.-B.; Wei, S.-L.; Ma, T.-F. Vapor phase assembly of benzotriazole and octadecylamine complex films on aluminum alloy surface. *J. Coat. Technol. Res.* **2020**, *18*, 435–446.
26. Goncharova, O.A.; Luchkin, A.Y.; Kuznetsov, Y.I.; Andreev, N.N.; Andreeva, N.P.; Vesely, S.S. Octadecylamine, 1,2,3-benzotriazole and a mixture thereof as chamber inhibitors of steel corrosion. *Int. J. Corros. Scale Inhib.* **2018**, *2*, 203–212.
27. Luchkin, A.; Goncharova, O.; Arkhipushkin, I.; Andreev, N.; Kuznetsov, Y. The effect of oxide and adsorption layers formed in 5-Chlorobenzotriazole vapors on the corrosion resistance of copper. *J. Taiwan Inst. Chem. Eng.* **2020**, *117*, 231–241. [[CrossRef](#)]
28. Luchkin, A.Y.; Goncharova, O.A.; Andreeva, N.P.; Kasatkin, V.E.; Vesely, S.S.; Kuznetsov, Y.I.; Andreev, N.N. Mutual Effects of Components of Protective Films Applied on Steel in Octadecylamine and 1,2,3-Benzotriazole Vapors. *Materials* **2021**, *14*, 7181. [[CrossRef](#)] [[PubMed](#)]
29. Kazanskii, L.P.; Selyaninov, I.A. XPS of 1,2,3-benzotriazole nanolayers formed on iron surface. *Prot. Met. Phys. Chem. Surf.* **2010**, *46*, 797–804. [[CrossRef](#)]
30. Goncharova, O.A.; Luchkin, A.Y.; Senchikhin, I.N.; Makarychev, Y.B.; Luchkina, V.A.; Dement'eva, O.V.; Vesely, S.S.; Andreev, N.N. Structuring of Surface Films Formed on Magnesium in Hot Chlorobenzotriazole Vapors. *Materials* **2022**, *15*, 6625. [[CrossRef](#)] [[PubMed](#)]
31. Petrunin, M.A.; Maksaeva, L.B.; Yurasova, T.A.; Terekhova, E.V.; Maleeva, M.A. The Effect of SelfOrganizing Vinyl Siloxane Nanolayers on the Corrosion Behavior of Aluminum in Neutral ChlorideContaining Solutions. *Prot. Met. Phys. Chem. Surf.* **2014**, *50*, 784–791. [[CrossRef](#)]
32. Petrunin, M.A.; Maksaeva, L.B.; Yurasova, T.A.; Terekhova, E.V.; Maleeva, M.A.; Kotenev, V.A.; Kablov, E.N.; Yu, A. Formation of Organosilicon Self-Organizing Nanolayer on an Iron Surface from Vapor Phase and Their Effect on Corrosion Behavior of Metal. *Prot. Met. Phys. Chem. Surf.* **2015**, *51*, 1010–1017. [[CrossRef](#)]

**Disclaimer/Publisher's Note:** The statements, opinions and data contained in all publications are solely those of the individual author(s) and contributor(s) and not of MDPI and/or the editor(s). MDPI and/or the editor(s) disclaim responsibility for any injury to people or property resulting from any ideas, methods, instructions or products referred to in the content.